Available online at www.sciencedirect.com
ScienceDirect
Journal of Photochemistry and Photobiology A: Chemistry 197 (2008) 197–205
Journal of Photochemistry and Photobiology A:Chemistry
www.elsevier.com/locate/jphotochem

Photo-induced self-cleaning and biocidal behaviour of titania and copper oxide multilayers

H.M. Yates [a,*], L.A. Brook [a], I.B. Ditta [b], P. Evans [a], H.A. Foster [b], D.W. Sheel [a], A. Steele [b]

[a] *Institute for Materials Research, University of Salford, Manchester M5 4WT, UK*
[b] *Centre for Parasitology and Disease, Biomedical Sciences Research Institute, University of Salford, Manchester M5 4WT, UK*

Received 27 November 2007; received in revised form 20 December 2007; accepted 26 December 2007
Available online 5 January 2008

Abstract

This paper describes the deposition of films of titania and copper oxide by atmospheric pressure chemical vapour deposition (CVD). The films were investigated as part of multilayer systems to assess their potential to offer the dual functionality of self-cleaning and biocidal films. The multilayer systems were achieved by deposition of copper oxide with subsequent titanium dioxide deposition and vice versa. Two different CVD approaches were employed in combination, thermal CVD and flame-assisted CVD. It is shown that by careful choice of the experimental growth conditions, multilayers can be formed with both biocidal and 'self-clean' functionality under UV photo-induced conditions.

Keywords: Titania; Copper oxide; Photo-activity; Biocidal; Chemical vapour deposition

1. Introduction

The self-cleaning properties of TiO_2 are well known and arise from its photocatalytic and hydrophilic nature, which has been the subject of much previous research. Applications have included self-clean glazing products [1], air (and water) purification [2] and antibacterial systems [3]. Although TiO_2 does have some biocidal activity it is much enhanced on addition of other species such as silver [4] or copper.

Copper is used in many commercial products such as fungicides [5] and anti-fouling paints [6]. Recognition of its beneficial health effects stretch back to the Roman Empire where it was realised that copper cooking utensils helped to prevent the spread of disease. More recently copper cations have been shown to be biocidal by their control of various bacteria including *Legionella* [7], *Listeria monocytogenes* and methicillin resistant *Staphylococcus aureus* (MRSA) [8,9]. The bacterial killing is believed to take place via copper ions. The ions bind to specific sites in the DNA (in the bacteria cells) [10] favouring guanosine residues [11]. This causes single strand breaks and base modification. Studies have shown that hydrogen peroxide has no effect on its own, but in the presence of copper ions can enhance the process [12]. Use of free radical scavengers reduces the reaction, so suggesting that they are involved [13]. As the photocatalytic behaviour of TiO_2 is believed to proceed via formation of hydrogen peroxide and free radicals [14] the combination of Cu–TiO_2 is an attractive one, which could enhance the biocidal activity of the material. Combined sol–gel produced TiO_2 plus copper have previously been reported as showing enhanced killing of *E. coli* [15] and *Staphylococcus epidermidis* [16] compared to TiO_2 alone. One possible mechanism involves the partial decomposition of the bacterial cell outer membrane by a photocatalytic process, followed by permeation of the copper ions into the cytoplasmic membrane causing disruption [15,17]. *S. epidermidis* has properties similar to MRSA, which is of serious concern in hospitals today, but is much safer to handle. In previously published work [18] we have shown that silver added to titania (grown by CVD) significantly enhances biocidal properties. The use of copper offers alternatives, or complimentary capability (e.g. to reduce chances of resistance or resistance development).

Along with improvements in bioactivity the self-clean functionality of the TiO_2 should be able to remove the dead cells (and any other pollutants) allowing the process to be repeatable. These combined advantages increase the potential commercial uses of these materials.

* Corresponding author. Tel.: +44 161 295 3115; fax: +44 295 5111.
E-mail address: H.M.Yates@salford.ac.uk (H.M. Yates).

1010-6030/$ – see front matter © 2008 Elsevier B.V. All rights reserved.
doi:10.1016/j.jphotochem.2007.12.023

In this paper we report on the growth and characterisation of these multilayered films. This includes discussion on the modifications necessary to the growth conditions, in order to produce truly multifunctional films with both photocatalytic and biocidal properties.

2. Experimental

2.1. Growth

All films were grown on pre-coated (CVD) silica-coated barrier glass substrates. The TiO_2 films were grown using an atmospheric pressure thermal CVD coater. The precursor for titania growth was titanium tetraisopropoxide, TTIP, (7.79×10^{-4} mol min^{-1}) (Aldrich) transported to the reactor by 0.5 l min^{-1} N_2 via a bubbler. The substrate temperature for growth was set to 500 °C. The total gas flow was 11 l min^{-1}. The CuO films were grown using an atmospheric pressure flame-assisted CVD coater with a propane/oxygen flame, described in detail previously [19]. The substrate temperature was set at 400 °C. An aqueous solution of 0.5 M $Cu(NO_3)_2$ was nebulised, into a carrier of N_2, through the flame and onto the substrate.

2.2. Characterisation

The crystallinity and structure of the samples was assessed by X-ray diffraction (Siemens D5000). The morphology of the samples was obtained by SEM (Philips XL30 FEGSEM) and atomic force microscopy (NanoScope IIIa, Digital Inst. Ltd.). X-ray photoelectron Spectroscopy (XPS; Kratos AXIS Ultra) with an Al (monochromated) Kα radiation source was used to check the surface composition and stoichiometry of the films. It was necessary to use a charge neutraliser as all the samples were insulating, due mainly to the deposition on glass. This tends to shift the peak positions up to 2 eV so the measurements were referenced to the residual C 1s signal at 285 eV. Curve fitting with CASA XP software using a mixture of Gaussian–Lorentzian functions was used to deconvolute spectra. Rutherford backscattering was also used to assess the bulk stoichiometry and layer positioning (within the multilayer samples) using an analyzing beam of 2 MeV He^+ with the sample being analysed at normal incidence with a scattering angle of 168° in IBM geometry.

Photocatalytic behaviour was measured under UV (365 nm, 3 mW cm^{-2}). The degradation of stearic acid (100 μl of 10 mmol in methanol) was followed by FTIR (Bruker, Vector 22). The technique used [20] was developed from work described previously [21–23]. The activity rates given are calculated from straight-line fits which give numerical values for comparisons. For bioactivity testing a modification of the standard test described by BS EN 13697:2001 was used [16]. The procedure for sterilisation of coated samples before biocidal activity testing was to shake the samples for 40 min in 100% methanol. Samples were removed aseptically and placed in a UVA transparent disposable plastic Petri dish, film side uppermost. The coated samples were then pre-irradiated by placing them under a 40 W UVA bulb with a 2.24 mW cm^{-2} output for 24 h.

E. coli ATCC 10536 and *S. epidermidis* NCTC 11047 were subcultured into Nutrient Broth (Oxoid, Basingstoke, UK) and inoculated onto Cryobank beads (Mast Diagnostics, Liverpool, UK) and the plate stored at −70 °C. Beads were subcultured onto nutrient agar (Oxoid) and incubated at 37 °C for 24 h and stored at 5 °C. A 50 μl loopful was inoculated in to 20 ml isosensitest broth (Oxoid) and incubated for 24 h at 37 °C. Cultures were centrifuged at 5000 × *g* for 10 min in a bench centrifuge and the cells were washed in de-ionised water three times by centrifugation and re-suspension. Cultures were re-suspended in water and adjusted to OD 0.5 at 600 nm in a spectrophotometer (Camspec, M330, Cambridge, UK) to give approximately 2×10^8 colony forming units (cfu) ml^{-1} which were inoculated on to each test sample and spread out using the edge of a flame-sterilized microscope cover slip.

The prepared samples were then UV activated. Four samples were exposed to three 15 W UVA lamps at 2.29 mW cm^{-2}. At time zero, a sample was removed immediately and the remaining samples removed at regular intervals. Four samples exposed to UVA but covered with a polylaminar UVA protection film (Anglia Window Films, UK) to block UVA but not infra-red, acted as controls.

The samples were then immersed in 40 ml of sterile de-ionised water and vortexed for 60 s to re-suspend the bacteria. A viability count was performed by serial dilution and plating onto nutrient agar in triplicate and incubation at 37 °C for 48 h. Each experiment was performed in triplicate.

For the elution tests sterilized distilled water was inoculated onto aseptically prepared samples. These samples were irradiated for fixed periods of time under UV (365 nm, 2.24 mW cm^{-2}) and then removed. The containers were then flooded with 9800 μl sterile water and agitated. The fluid was then aseptically decanted into a sterile plastic bottle and 100 μl concentrated nitric acid added to make sure all the Cu was in solution, before ICPMS analysis.

3. Results and discussion

In order to understand the influence of the various layered structures, several types of film were produced and characterised. Multilayers of TiO_2 with an underlayer of CuO (TiO_2 on CuO on SiO_2-coated glass) and the inverse (CuO on TiO_2 on SiO_2-coated glass) were grown. The properties of the multilayers were referenced to individual layers of TiO_2 and CuO on glass grown under identical conditions to the multilayer composites.

Two CVD methods were employed as it was not possible to deposit dense coherent thin (anatase) TiO_2 films by FACVD. This arises from the reactivity (in the flame) of available precursors, leading to the production of TiO_2 powder (or a low density agglomerated film) on the surface of the substrate. The proposed reason for this is associated with the same property that makes FACVD such an attractive alternative to conventional APCVD, i.e. the ability of the flame to provide a highly energised environment that can initialise precursor decomposition, including materials that could otherwise not be utilised as conventional CVD precursors due to their low volatility (e.g. $Cu(NO_3)_2$).

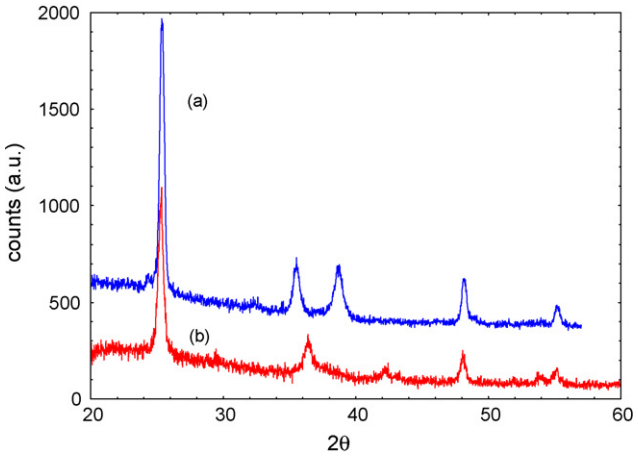

Fig. 1. XRD of (a) CuO over TiO_2 and (b) TiO_2 over CuO.

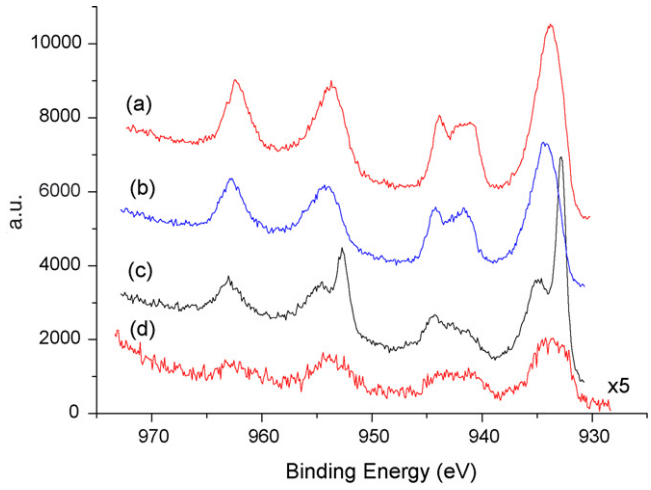

Fig. 2. High-resolution XPS Cu 2p spectra for (a) CuO over TiO_2, (b) CuO, (c) TiO_2 over a thick CuO layer and (d) TiO_2 over a thin CuO layer.

As yet there are no reports in the literature that give suggested decomposition pathways for precursors in FACVD processes. This is in contrast to other CVD process such as the thermal APCVD of TTIP, which was successful in this work. The reaction of TTIP has been extensively studied in the literature and has been shown to proceed via intra- or intermolecular decomposition pathways depending on the conditions used [24,25].

3.1. Visual

All films were well adhered to the glass substrate and transparent. Single layers of TiO_2 had interference fringe colours relating to the thickness, while single layers of CuO appeared yellow-brown in reflected light. Single reference films were 61 nm and 13 nm for the CuO and 80 nm for the TiO_2.

3.2. X-ray diffraction

All deposition was shown to be polycrystalline, as seen in Fig. 1. Both growths of TiO_2 above and below CuO was in the form of anatase (JCPDS 21-1272), with the main signals at 25°, 48° and 55°, corresponding to (1 0 1), (2 0 0) and (2 1 1) orientations. When CuO was deposited above the TiO_2 layer, copper II oxide (JCPDS 45-0937) was formed with a diffraction pattern identical to that of a single layer of CuO. The two main signals centred round 35° ((0 0 2), (−1 1 1)) and 39° ((1 1 1), (2 0 0)).

However, when TiO_2 was grown over a 61-nm thick CuO layer the final result (Fig. 1(b)) showed that the CuO present was now in the form of Cu I oxide (JCPDS 05-0667) with signals at 29° (1 1 0), 36° (1 1 1) and 42° (2 0 0). For TiO_2 deposited over the much thinner CuO (13 nm) film, the copper oxide related signals could not be seen, mostly likely due to insufficient CuO present to detect, either in the sample or near the surface.

Use of Scherrers formula [26] allows calculation of crystallite size. The calculation is ideally for a powder not a thin film, so will contain line width broadening from strain as well as crystallite size. Despite these reservations the values obtained will give an idea of the changes occurring. Growth of TiO_2 over a thin CuO layer does not lead to any significant change in anatase crystallite size (45 nm opposed to 47 nm), while growth on the thicker CuO layer leads to a reduction in size to 30 nm. This reduction in TiO_2 crystallite size reflects the much rougher surface for deposition with the latter, thicker CuO sample, as shown later.

From XRD it is not possible to confirm whether the multilayered samples consist of two distinct layers or a mixture of materials on the surface. In order to determine the nature of the surface it was necessary to turn to XPS, as this is surface sensitive, only penetrating approximately the first 5 nm of the sample.

3.3. X-ray photoelectron spectroscopy

Fig. 2 shows the Cu 2p high-resolution spectra for both multilayers and a single layer of CuO. These consist of the $2p_{3/2}$ and $2p_{1/2}$ along with shake-up satellite peaks. Those for the CuO over TiO_2 (Fig. 2(a)) and a single layer of CuO (Fig. 2(b)) are identical and can be identified as copper II oxide. The $2p_{3/2}$ is at 934.4 eV with a splitting of 19.8 eV [27]; along with high intensity of the shake-up satellites [28] (at 943 eV and 963 eV) confirm the assignment.

Spectra for the nominally TiO_2 over CuO sample (Fig. 2(c)) is different, consisting of two sets of 2p signals and hence two chemically different species of Cu. Curve fitting of this led to the assignment of the $2p_{3/2}$ at 932.8 eV to Cu I oxide [29] and that at 934.5 eV to that of Cu II oxide as before. A signal from the Cu I oxide is expected to be narrower than that of the Cu II oxide [28]. The more intense signal from Cu I oxide has a narrower line-width, 1.54 eV, than that of the Cu II oxide signal, 3.41 eV, which is in agreement with the assignment made.

The high-resolution Ti 2p spectra for the TiO_2 over CuO sample (Fig. 3(a)) show the Ti 2p at $p_{3/2} = 458.8$ eV. This along with the position of the O 1s (530.7 eV) (not shown) confirmed that this was TiO_2 [30]. However, it is only a weak signal suggesting that there is little TiO_2 on the surface. The positions of the Ti 2p and Cu 2p are not shifted in comparison to single layers, so suggest that the species are chemically distinct. No signal for Ti was seen for the CuO over TiO_2 sample (Fig. 3(b)) confirming a lack of detectable pinholes.

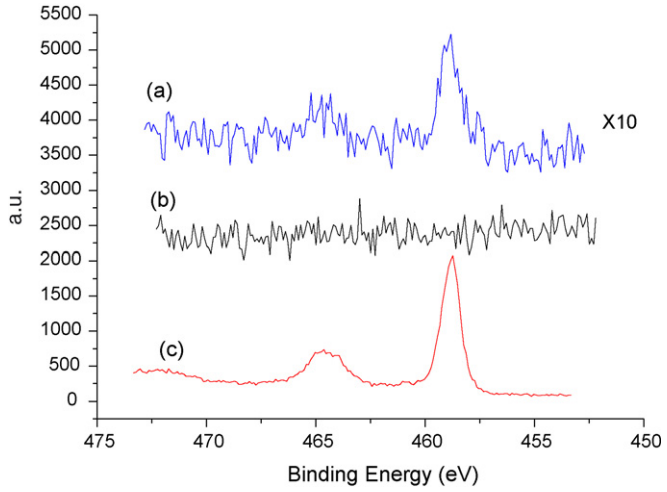

Fig. 3. High-resolution XPS of Ti 2p for (a) TiO_2 over a thick CuO layer, (b) CuO over TiO_2 and (c) TiO_2 over a thin CuO layer.

The above results were for TiO_2 deposited over a thick layer of CuO. If a much thinner layer of CuO was used as the under layer, the resulting XPS was different. In this case the Cu 2p signal (Fig. 2(d)) was that of copper II oxide, and of lower intensity compared to the previous multilayer, while the Ti 2p signal was much stronger (Fig. 3(c)). This suggests that there was now much more TiO_2 and less CuO on the surface.

Returning to the sample of nominally TiO_2 over a thick CuO layer, it was a surprising finding that on the addition of the TiO_2 layer, not only that the Cu ions migrated to the surface, but also that it now contained Cu_2O as well as CuO. The presence of Cu on the surface is most likely due to the relatively high growth temperature of the TiO_2, which enhanced the fast diffusion of Cu through the growing layer. That there is some Cu_2O formed may be due to the presence of a slightly sub-stoichiometric TiO_2 layer, so that the Ti^{4+} ions could act as gettering species removing oxygen from the CuO, leading to the formation of the more copper-rich Cu_2O oxide. Due to the weak Ti 2p signal (and hence increased error in fitting) it was not possible to accurately determine any slight sub-stoichiometry and hence confirm the hypothesis.

3.4. Rutherford back scattering

For further details of the samples bulk stoichiometry and information about the ordering of the samples RBS analysis was applied. The spectrum will only show a distinct peak for an element if it exists only in a specific position within the sample. For example, O exists as a rising edge as it is present throughout the deposited layers and the substrate. However, both Ti and Cu can be seen as distinct peaks. If they were on the surface they would lie at 287 and 310 respectively, but would move to lower channel numbers if present under the surface. The amount

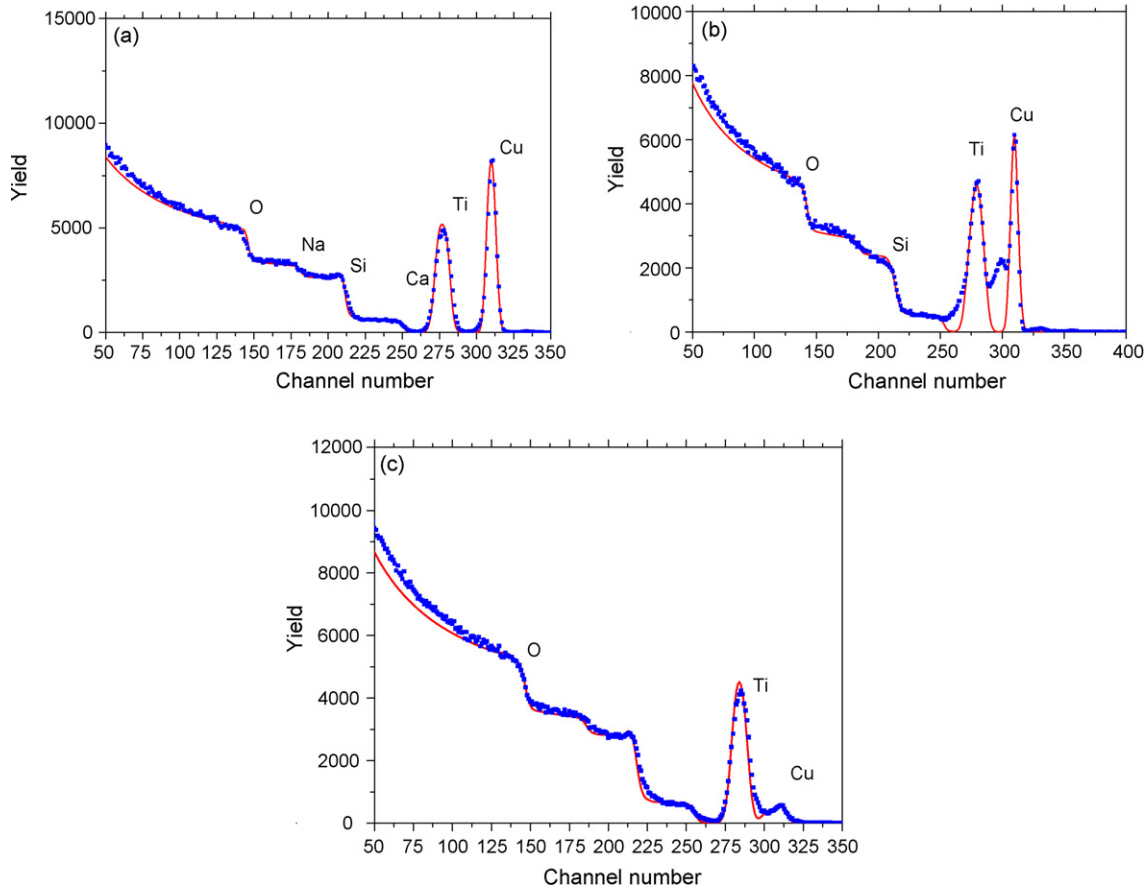

Fig. 4. RBS of (a) CuO over TiO_2, (b) TiO_2 over CuO (thick layer) and (c) TiO_2 over CuO (thin layer).

of shift is dependent on the thickness and density of the upper layer.

Fig. 4(a) shows the RBS spectrum of a multilayer of CuO deposited over TiO_2. As can be clearly seen the Ti and Cu still exist as distinct layers with any mixing below the detection level of the RBS. As expected the Cu signal showed no shift while that of the Ti signal has shifted to lower channel numbers confirming the layered structure was that originally deposited. Calculations established that the layers consist of stoichiometric CuO, TiO_2 and SiO_2 (from the substrate barrier layer).

Fig. 4(b) shows the RBS spectrum of a multilayer of TiO_2 grown over a thick layer of CuO. From this data it can be seen that the Ti signal (at channel numbers 277) and not the Cu, signal (at channel number 310) has shifted. This implies that there is mainly Cu on the surface with Ti underneath. The signal at channel 299 and the high background yield to channel numbers between the Ti and Cu signals were considered to be related to mainly Cu species under the surface at different depths, along with a small contribution from Ti nearer the surface (up to channel 287). Calculations gave a surface ratio of $Cu_{3.3}O_{0.5}Ti_{1.2}$, which would fit with the previously discussed XPS and XRD data of a Cu I oxide surface with a small amount of TiO_2.

The RBS of a multilayer grown of TiO_2 over a thin layer of CuO (Fig. 4(c)) shows signals for both Cu (channel number 310) and Ti (channel number 285), so confirming the XPS data in that there is now a surface layer containing TiO_2 doped with Cu. Calculations of the stoichiometry establishes that the film consists of a layer of TiO_2 with a concentration gradient of Cu through out. Again this is of greatest concentration on (and as calculated within 30 nm of) the surface (elemental ratio $TiO_{2.4}Cu_{0.08}$). Due to the migration of the Cu atoms through the film there is now no distinct separate film relating to CuO. Modelling the data led to a thickness for this layer of 70 nm. This is smaller than that measured for the growth of two individual layers (TiO_2 80 nm and CuO 13 nm). However, as judged by the nano-particulate nature of the films (see Section 3.5) the density of the films is less than that of the bulk densities. A reduction in the density used in modelling would lead to a greater sample thickness.

3.5. Morphology

3.5.1. Scanning electron microscopy

The SEM image of CuO deposited by FACVD showed an island growth-type structure of packed spherical nanoparticles, while that of a single TiO_2 layer, although particulate in nature looks much smoother. Growth of CuO over TiO_2 (Fig. 5(a)) established that the upper layer, although still CuO, was very dissimilar in appearance to that of a single CuO layer (Fig. 5(c)). The surface morphology looking more like that of the TiO_2 single layer, suggesting the CuO deposition was very much influenced by the underlying structure, in this case a change from amorphous smooth silica to crystalline titania.

The TiO_2 over CuO (thick) sample (Fig. 5(b)) had a much more pronounced particulate structure than the other surfaces. As the TiO_2 deposition is on a rough, nano-particulate surface an uneven almost nano-particulate final surface is not surprising. As established earlier the actual surface layer in this sample is

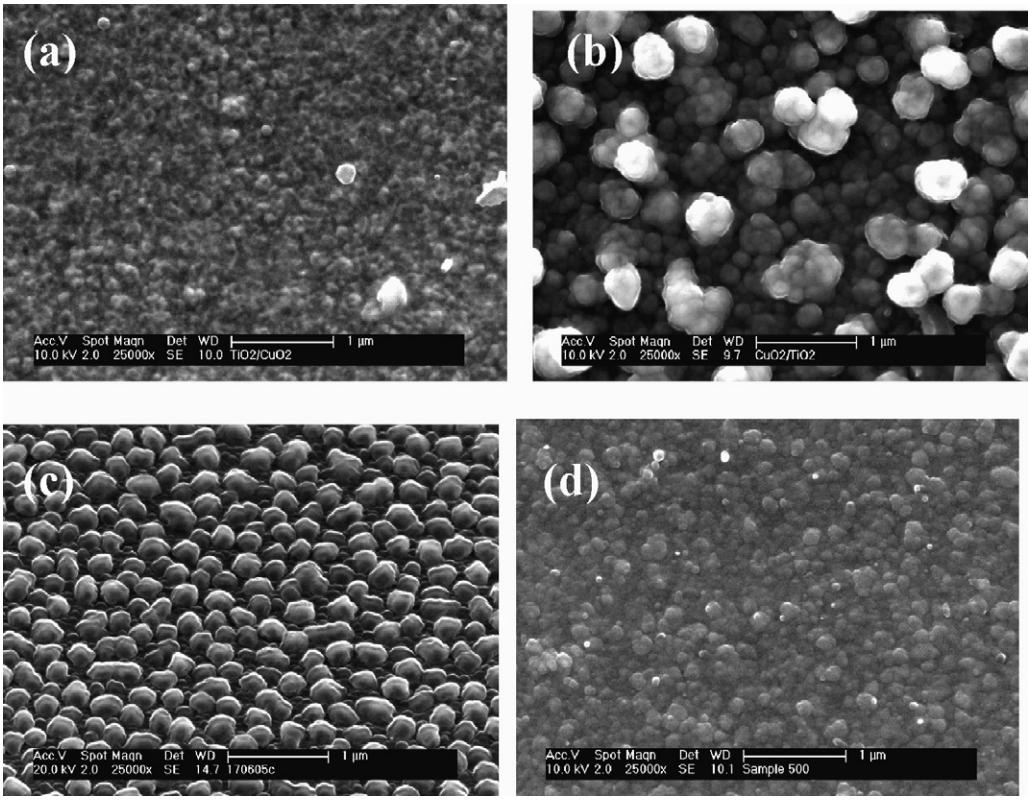

Fig. 5. SEM images of (a) CuO over TiO_2, (b) TiO_2 over CuO, (c) CuO and (d) TiO_2.

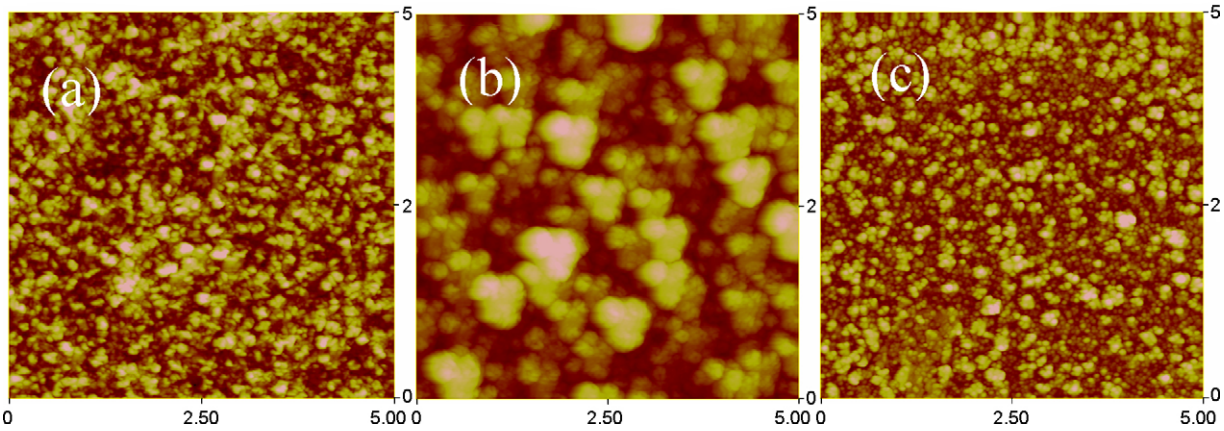

Fig. 6. AFM images (5 μm × 5 μm) (a) CuO over TiO_2, (b) TiO_2 over (thick) CuO and (c) TiO_2 over (thin) CuO.

mainly Cu_2O with some TiO_2, so as the final species are different the change in morphology could be expected.

3.5.2. Atomic force microscopy

Atomic force microscopy was used to examine the surface morphology in more detail. This confirmed that the higher magnification images of the surfaces mirrored that of the structure shown by SEM. Fig. 6(a) (CuO over TiO_2) shows a surface of small particulates over a depth of 100 nm, while that of TiO_2 over (thick) CuO (Fig. 6(b)) had much larger particulates over a depth of 300 nm. That of the TiO_2 over the thinner CuO layer (Fig. 6(c)) showed a surface of relatively smaller particulates, compared to that deposited on the thicker CuO layer. These surface features were more in line with the morphology expected for a single TiO_2 surface of similar thickness.

In addition the roughness of the surface was quantified by a Ra measurement over an area of 5 μm × 5 μm. That of the TiO_2 over the thicker CuO layer (Ra = 41 nm) being similar to that of a single CuO layer (Ra = 39 nm) as expected, as generally deposition over a rough surface will accentuate the features. CuO over TiO_2 had a value (Ra = 11 nm) closer to that of a single TiO_2 layer (Ra = 9 nm). Deposition of TiO_2 on the much thinner (and smoother) CuO layer (Ra = 12 nm) showed no significant change in roughness from that of a single layer of the thinner CuO (Ra = 7 nm). All these values again suggest that the morphology of the upper layer depended strongly on the under layer.

3.6. Functional properties

3.6.1. Photo-activity

Three experiments were run for each type of sample and the average activity rate taken. For CuO over TiO_2 and TiO_2 over the thicker CuO layer the rates were moderate at 0.0020 cm^{-1} min^{-1} and 0.0015 cm^{-1} min^{-1}, respectively. These values are very similar to that of a single layer of CuO, which gave an activity rate of 0.0017 cm^{-1} min^{-1}. This all fits with the earlier conclusion that the top surface in both multilayered samples is mainly a Cu oxide. Interestingly, Colon et al. [31] suggests that Cu^+ is needed for improved photo-activity, rather than Cu^{2+} in TiO_2 systems doped with Cu. However, no change in rate values was seen here suggesting that the oxidation state of the copper was not making an obvious difference in terms of photo-activity.

From Fig. 7 it can be seen that a sample of TiO_2 deposited over a thin CuO layer, which was considered to have a surface of Cu^{2+}-doped TiO_2 gave an improved photo-activity, over that of a single layer of CuO. The increased rate of 0.0031 cm^{-1} min^{-1} is probably directly related to the presence of photo-active TiO_2 on the surface. Although, this was lower than the rate value obtained for a single reference layer of TiO_2 grown directly on to barrier glass under identical conditions (0.005 cm^{-1} min^{-1}) it was still at a reasonable level for commercial exploitation. For example, one commercial 'self-clean' glass tested under our experimental conditions gave a rate of 0.0030 cm^{-1} min^{-1}. Also, in spite of the apparent reduction in photo-activity of this multilayer its usefulness should be considered alongside the additional biocidal functionality, as discussed below (Section 3.6.2).

3.6.2. Biocidal activity

The *E. coli* killing rate for CuO over TiO_2 showed a >5 log reduction over 40 min (Fig. 8(a)), compared to the control sample which showed no change. That of the nominally TiO_2 over CuO was faster and took a maximum of 20 min (Fig. 8(b)). Comparisons of biocidal rate to that of reference thick CuO samples (3–7 min), shows that the rate has been reduced upon inclusion in a multilayer. Previous results from tests on TiO_2 [18] established that it was biocidal, although to a much lower degree (>log 5 reduction between 180 and 240 min).

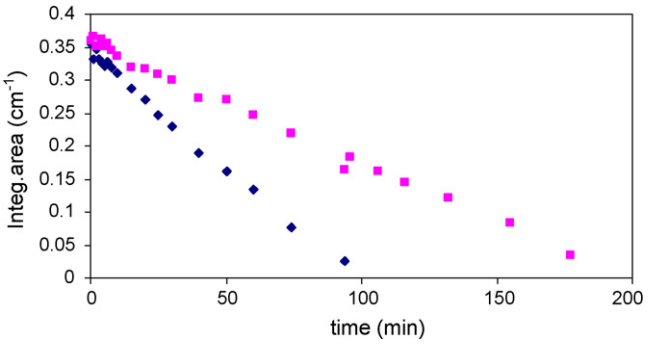

Fig. 7. Photo-activity of (a) ■ CuO, (b) ◆ TiO_2 over a thin CuO layer.

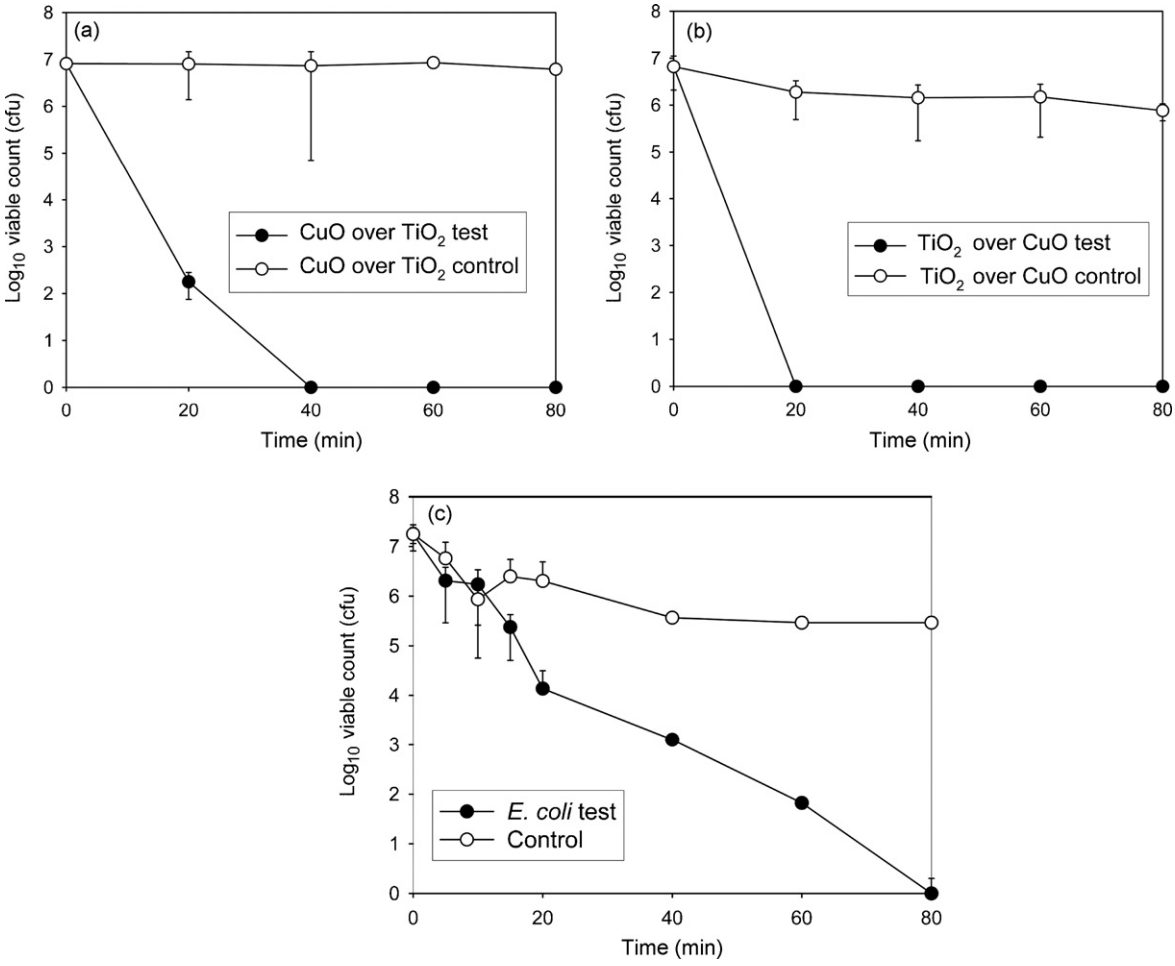

Fig. 8. Graphs showing the killing rate of *Escherichia coli* for (a) CuO over TiO_2, (b) TiO_2 over CuO (61 nm) and (c) TiO_2 over CuO (13 nm). The error bars give the standard deviation for the results of three experiments on each set of samples.

The earlier analysis in this paper established that the TiO_2 over the thicker CuO layer had a mixed species surface layer of mainly Cu I oxide with some Cu II oxide, along with a very small amount of TiO_2. The bio-activity of this combined film lies closer to the single film CuO values than that of the other samples. This is not surprising as the surface is mainly a copper oxide. However, little difference in bioactivity was noted (due to the limitations on sampling time resolution) between films containing mainly Cu^{2+} (single CuO films) and Cu^{+} (nominal TiO_2 over thick CuO). The TiO_2 present on the surface could be either an advantage (via catalyzing the copper mediated site specific DNA damage [32]) or a disadvantage (as TiO_2 has a much lower bioactivity rate). Considering the very small trace of TiO_2, its effect on the bioactivity will be very slight.

The bioactivity of the sample of TiO_2 with an overlayer of CuO is lower than that of a reference CuO sample. The various characterisations shown earlier do not show any difference in the chemical nature of the samples. However, it has a very different surface morphology, to that of a single CuO layer, as seen by the SEM images of much smoother and smaller particle sizing. This suggests that the nano-particulate structure, which gives its greater surface area, is of importance and may affect the amount of Cu released from the surface.

The final biocidal tests were with the TiO_2 layer over a thin CuO layer (Fig. 8(c)), which had been shown to have a surface area of mainly TiO_2 with a very small amount of CuO. Although these multilayers are of lower bio-activity than the previous CuO/TiO_2 samples with >5 log reduction over 80 min, there was much less Cu on the surface and the value is much improved to that of just TiO_2, giving added functionality to the TiO_2 layer. This is comparable to results we previously published for TiO_2 over Ag, in which > 5log reduction over 60 min was obtained [16].

These results are all for biocidal activity (as described by the method in Section 2.2) in the presence of UV light. Some testing was also carried out in the dark without the presence of UV light. Results showed that only very limited activity occurred with, for example, the sample of TiO_2 over the thick CuO layer showing a 1 log reduction over 80 min in comparison to a >5 log reduction over 20 min under UV.

As discussed in the introduction, it is considered that the major killing effect is due to Cu ions. To determine if any Cu ions were present elution tests were carried out. In these tests the samples were treated as if undergoing a bacterial test, but water and no bacteria added. After set times (under UV) additional water was added and then withdrawn. This fluid was checked

by ICPMS for its Cu content. All samples tested showed the presence of Cu ions in the eluted fluid, values ranging from 2 to 8 ppm, depending on the exact sample and time of extraction. A total period of 80 min was chosen, as it was greater than the time period shown to be needed for total kill of the bacteria. The CuO over TiO_2 and CuO samples gave relatively similar values, averaging 3.3 and 2.8 ppm, respectively over the total period. While the nominally TiO_2 over the thick copper layer averaged 5.5 ppm. Although the kill mechanism depends on the Cu ions, it cannot be a direct relationship between the concentration of Cu ions in solution and an increased kill rate, as both trends are different. This would imply that other factors such as the roughness of the film (surface area for interaction, ease of spreading of the bacteria over the surface and of removing them for sampling) need to be taken into consideration.

3.6.3. Functional regeneration

Once the bio-test had been carried out the surface is visibly coated with dead bacteria. For the surface to continue to be used as a biocidal surface the dead bacteria need to be removed. Due to the UV photo-activity of the TiO_2 this was proved possible. The used samples were exposed to UV light and the concentration of the organic material monitored by FTIR. As shown in Fig. 9, the 'self-clean' nature of the surface could remove the remaining pollutants under 30 min.

As an additional test, samples previously used for biocidal testing of the TiO_2 over a thin CuO layer were utilised for a further set of biocidal tests (having already been used three times each). The average of three tests with these samples with *E. coli* and *S. epidermidis* were carried out, as shown in Fig. 10.

As can be seen the samples were still bioactive with a 2 log reduction in 60 min. This was lower than that achieved by the results shown in Fig. 8c. However, it must be stated that these samples had been repeatedly used for over nine experiments for which it was necessary to clean stringently to allow accurate biocidal experimentation and this led to deterioration of the films in some cases. One important point to note is that both *E. coli* and *S. epidermidis* were killed at similar rates. Gram-positive bacteria such as *S. epidermidis* are generally considered to be more resistant than Gram-negative bacteria such as *E. coli* [33,34] but in this case there was little difference. In addition, the presence of the self-cleaning properties, from the TiO_2, may be an advantage over solely Cu surfaces, which can become fouled in "in use" simulations [35]. The addition of the TiO_2 to the CuO could help to prevent the fouling of the CuO surface.

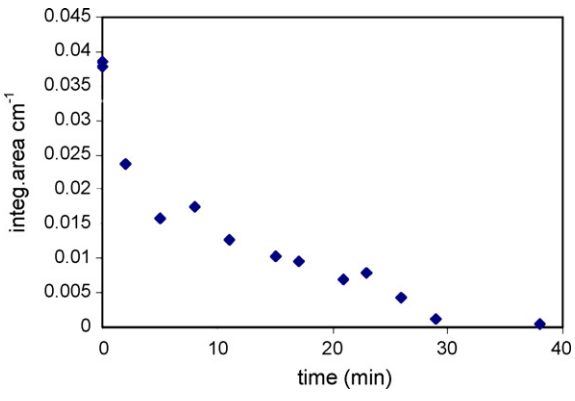

Fig. 9. Graph showing the removal of the dead bacteria over time under UV.

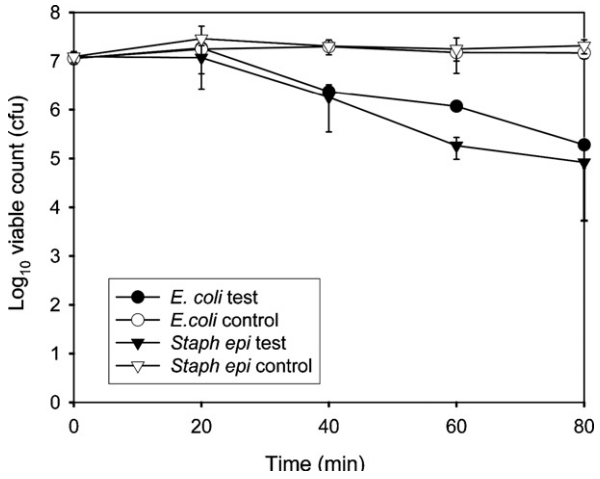

Fig. 10. Graph showing the killing rate of *E. coli* and *S. epidermidis* for TiO_2 over CuO (13 nm). The error bars give the standard deviation for the results of three experiments on each set of samples.

4. Summary

By use of a sequential method of FACVD and thermal CVD it was possible to deposit thin films of polycrystalline titania and copper oxide as dual layer structures. In both cases the titania forms as anatase. When copper oxide is deposited on top of titania it forms as copper II oxide, which is the form when deposited directly on glass under the same experimental conditions. This layer is formed without detectable pinholes, as established by XPS. However, when TiO_2 was deposited on top of copper II oxide (61 nm thick), there is a rapid migration of Cu to the top surface due to the high growth temperature. This left a top surface consisting mainly of copper I oxide, with a trace of TiO_2.

Photocatalytic UV measurements, by the stearic acid test, gave moderate activity in all cases, similar to that of a single CuO layer. As all the surfaces were mainly of copper oxide, this is perhaps predictable. By a change of the growth procedure to produce a much thinner under layer of CuO, it was also possible to obtain multilayers with mainly TiO_2 on the surface. These proved more photo-active under UV radiation, than the CuO-related counterparts and comparable to commercially available TiO_2 films.

Under UV photo-induced conditions biocidal testing with *E. coli* established that having Cu oxide on the surface of the multilayer was not as active as that of a single CuO layer, although still highly active. The reduction is considered due to the change in the morphology, from a nano-particulate to a smoother surface of small particles. This lower surface area having an adverse effect.

The nominally TiO_2 over a thick CuO layer had a bioactivity closer to that of the single CuO layer, which was as attributed to the surface being mainly CuO. Use of a thinner underlayer of CuO, gave a film with a very low level of CuO on the surface which was sufficient to much improve the bioactivity over that

of a non-doped TiO_2 film and hence giving added functionality and possible commercial exploitation. Interestingly, testing of this particular type of sample was found to also have a biocidal effect, of similar level, with both Gram-negative *E. coli* and Gram-positive *S. epidermidis*. Further work is in progress to study this more closely.

In summary, multilayer, multi-deposition technology CVD approaches to CuO/TiO_2 layers show promising biocidal properties and a "self-regeneration" capability. Such layers may find application in areas requiring infection control.

Acknowledgements

This work was partly financed by the EC through GRD1-2001-40791, PHOTOCOAT project. We would like to thank M. Faulkner from University of Manchester Materials Science Centre for the SEM images and R. Valizadeh, Manchester Metropolitan University for the RBS data. Also, thanks to C. Liptrot and A. Mohammed, from the Biomedical Sciences Research Institute, University of Salford, for technical assistance with the biological tests.

The authors wish to acknowledge the EPSRC and Corus PLC for financial support for LB.

References

[1] http://www.Pilkington.com, http://www.Saint-Gobain.com.
[2] M.A. Fox, M.T. Dulay, Chem. Rev. 93 (1993) 341–357.
[3] Y. Kikuchi, K. Sunada, T. Iyoda, K. Hashimoto, A. Fujishima, J. Photochem. Photobiol. A 106 (1997) 51–56.
[4] M. Sökmen, F. Candan, Z. Sümer, J. Photochem. Photobiol. A 143 (2001) 241–244.
[5] G. Borkow, J. Gabbay, Curr. Med. Chem. 12 (2005) 2163–2175.
[6] T.E. Cooney, R.J. Tang, Methods Enzymol. 310 (1999) 637–644.
[7] J.E. Stout, Y.S. Lin, A.M. Goetz, R.R. Muder, Infect. Cont. Hosp. Epidemiol. 19 (1998) 911–914.
[8] H.T. Michels, S.A. Wilks, J.O. Noyce, C.W. Kneevil, Materials Science and Technology Conference, in: Copper for the 21st Century Symposium, Pittsberg, PA, September, 2005.
[9] J.O. Noyce, H. Michels, C.W. Keevil, Appl. Environ. Microbiol. 72 (2006) 4239–4244.
[10] R.B. Thurman, C.P. Gerba, CRC Crit. Rev. Environ. Cont. 4 (1989) 295–315.
[11] J.-L. Sagripanti, K.H. Kraemer, J. Biol. Chem. 264 (1989) 1729–1734.
[12] O.L. Aruoma, B. Halliwell, E. Gajewski, M. Dizdaroglou, Biochem. J. 273 (1991) 601–604.
[13] J.-L. Sagripanti, L.B. Routson, A.C. Bonifacino, C.D. Lytle, Antimicrob. Agents Chemother. 41 (1997) 812–817.
[14] A. Mills, S. Le Hunte, J. Photochem. PhotoBiol. A 108 (1997) 1–35.
[15] K. Sunada, T. Watanabe, K. Hashimoto, Environ. Sci. Technol. 37 (2003) 4785–4789.
[16] F. Heidenau, W. Mittelmeier, R. Detsch, M. Haenle, F. Stenzel, G. Ziegler, H. Gollwitzer, J. Mater. Sci. 16 (2005) 883–888.
[17] Y. Ohsumi, K. Kitamoto, Y. Anraku, J. Bacteriol. 170 (1988) 2676–2682.
[18] L.A. Brook, P. Evans, H.A. Foster, M.E. Pemble, A. Steele, D.W. Steel, H.M. Yates, J. Photochem. Photobiol. A 187 (2007) 53–63.
[19] M.J. Davis, G. Benito, D.W. Sheel, M.E. Pemble, Chem. Vapor Depos. 10 (2004) 29–34.
[20] H.M. Yates, M.G. Nolan, D.W. Sheel, M.E. Pemble, J. Photochem. PhotoBiol. A 179 (2006) 213–223.
[21] Y. Paz, Z. Luo, L. Rabenberg, A. Heller, J. Mater. Res. 10 (1995) 2842–2848.
[22] P. Sawunyama, L. Jiang, K. Hashimoto, J. Phys. Chem. B 101 (1997) 11000–11003.
[23] A. Mills, G. Hill, S. Bhopal, I.P. Parkin, S.A. O'Neill, J. Photochem. Photobiol. A 160 (2003) 185–194.
[24] S.-I. Cho, C.-H. Chung, S.H. Moona, J. Electrochem. Soc. 1489 (2001) 599–603.
[25] K.-H. Ahn, Y.-B. Park, W. Dong, Surf. Coatings Technol. 171 (2003) 198–204.
[26] B.D. Cullity, Elements of XRD, Addison-Wesley, 1978.
[27] J. Chastain, R.C. King, Handbook of X-ray Photoelectron Spectroscopy, Physical Electronic Inc., New York, 1995.
[28] S. Poulston, P.M. Parlett, P. Stone, M. Bowker, Surf. Interface Anal. 24 (1996) 811–820.
[29] J.P. Tobin, W. Hirschwald, J. Cunningham, Appl. Surf. Sci. 16 (1983) 441–452.
[30] Y.J. Sun, T. Egawa, L.Y. Zhang, X. Yao, Jpn. J. Appl. Phys. 41 (2002) L1389–L1392.
[31] G. Colon, M. Maicu, M.C. Hidalgo, J.A. Navio, Appl. Catal. B 67 (2006) 41–51.
[32] K. Hirakawa, M. Mori, M. Yoshida, S. Oikawa, S. Kawanishi, Free Radical Res. 38 (2004) 439–447.
[33] A. Pal, S.O. Pekhonen, L.E. Yu, M.B. Ray, J. Photochem. Photobiol. A 186 (2007) 335–341.
[34] H.-L. Liang Liu, T.C.-K. Yang, Process Biochem. 39 (2003) 475–481.
[35] P. Airey, J. Verran, J. Hosp. Infect. 67 (2007) 271–277.